Numerical Modeling of Rectangular Concrete-Filled Steel Tubular Short Columns

Heaven Singh, P.K. Gupta

Abstract— This paper presents a numerical investigation into the behavior of rectangular concrete filled steel tubular (CFT) short columns loaded in axial compression. Nonlinear finite-element analysis is performed for the compression process using commercial software ABAQUS 6.9 [1]. A total of 16 specimens of different steel tube sizes, wall thickness, length and filled with normal as well as high strength concrete are chosen for modeling from the available literature. The proposed model is validated by comparing its results with those of the corresponding experimental specimens. It is observed that the computational model is able to map the deformed shapes and the load deformation pattern of the CFT columns across different column sizes and filled with different grades of concrete. A good agreement is also observed between the experimental and predicted peak axial load capacities

Index Terms— ABAQUS, Axial Compression, CFT column, Confinement, Finite element, Peak axial load, Steel tube

1 INTRODUCTION

Concrete filled steel tubular (CFT) columns are a new type of structural member which are being extensively used across the world in construction of high-rise buildings, bridges etc. These compression members show higher axial load capacity, larger energy absorption, higher initial stiffness and better ductility than the conventional RC columns. These advantages are primarily due to the composite action between steel and concrete. The steel tube also acts as a formwork and supports the erection loads, thus reducing the overall cost [2].

In a CFT member, the confinement provided by the steel tube to the concrete core causes a triaxial stress state in concrete which is the main source of the enhanced compressive strength of the tubular columns. Many studies have been carried out to investigate the composite action in the CFT columns. Knowles and Park [3] observed that for circular columns, the peak load capacity was higher than the summation of individual load capacities of steel and concrete and could b predicted using the tangent modulus approach. A detailed study by Tomii et al [4] on 268 CFT columns concluded that the short columns failed mainly by crushing of concrete. Further, the circular and octagonal CFST columns were found to exhibit strain hardening or perfectly plastic post-yield behavior. But for square CFST columns, strain softening was the failure mode after the critical load was reached. Shakir- K halil [5] tested nine 3 m long in eccentric loading and twelve short rectangular specimens in concentric loading. Theyconcluded that BS 5400 [6] conservatively predicted the ultimate capacity of short columns in uniaxial bending about minor axis. Schneider [7] tested fourteen specimens to study the effect of tube shape and steel tube thickness on the composite column strength. It was observed that circular columns provided higher post-yield axial ductility and stiffness than square or rectangular columns. A finite element (FEM) analysis was also performed for these samples using the commercial code ABAQUS. Hu et al [8] also used the FEM program ABAQUS to simulate the behavior of composite columns in axial compression. Circular and square CFT members from Schneider [7] and Huang et al [9] were analysed. A good agreement was obtained between the numerical results and their experimental counterparts. Han [10] tested 24 rectangular CFT columns in compression. He concluded that the ultimate load capacity was influenced by confining factor and aspect ratio. Liu et al [11] tested 22 high-stength concrete filled CFT columns to failure under axial compression. These columns were found to present a similar failure behavior to the normal strength concrete filled specimens. Liu and Gho [12] also tested 26 high-strength rectangular columns and reported favorable ductility performance for all specimens. It was also observed that the local buckling in steel tube occurred firson the broader faces.

From the review of literature, it is clear that there is a lack of numerical FEM based model the experimental investigations for the rectangular CFT columns. Therefore, this paper primarily aims to present a numerical model for the analysis of such specimens. The model is then validated by comparison with some select experimental results from literature.

2 NUMERICAL MODELING METHOD

In a CFT member, the contact between steel tube and concrete causes composite action between the two members. The radial lateral confining pressure exerted by the steel tube on the concrete induces confinement in concrete. A biaxial state of stress is also induced in steel, which may cause some reduction in its axial load capacity. Thus any numerical model that intends to capture the behavior of CFT in compression must use suitable constitutive model for the steel tube and concrete.Further, to effectively replicate the inherent advantages of CFT, it is necessary that the composite action between steel and concrete be very carefully modeled.

2.1 Material Modeling

In the proposed model, the steel tube is modeled as an elastic-perfectly plastic material. The poisson ratio for steel is taken as 0.3. The values of Young's modulus E_s and yield strength f_y of the steel tube for different specimens given in Table 1 are used. Von-Mises yield criterion is used to define the yield surface for steel.

- *Heaven Singh is currently pursuing PhD degree program in civil engineering in Indian Institute of Technology (IIT) Roorkee, India. E-mail : heavensingh216@gmail.com*
- *P.K. Gupta is currently an Associate Professor in Department of civil engineering in IIT Roorkee,India. E-mail: spramod_3@yahoo.com*

The compressive strength of concrete is enhanced by the confinement provided by the steel casing. The confined concrete model adopted by Hu et al [8] is used to define the stress-strain behaviour for concrete in the modeling procedure. As per the method, the lateral confining pressure f_l is calculated as:

$f_l / f_y = 0.055048 - 0.001885(B/t)$ $(17 \leq B/t \leq 29.2)$ (1)

$f_l / f_y = 0$ $(29.2 \leq B/t \leq 150)$ (2)

$f_{cc} = f_c + k_1 f_l$ (3)

where f_c is the unconfined cylinder strength of concrete, f_{cc} is the confined strength of concrete and k_1 is a constant. A value of 4.1 is used for k_1 based on Richart et al [13]. B denotes the larger outer lateral dimension of the steel tube, while t represents the wall thickness of the tube.

Further, the Drucker Prager plasticity model inset in ABAQUS was adopted for specimens to describe the plastic stress strain behavior of the confined concrete.

2.2 Interface Modeling

The correct simulation of composite action between concrete and steel tube is the single most important factor guiding the behavior of the CFT column. To model this interaction, the normal contact between the two materials is provided using friction, with the inner surface of the stiffer steel tube serving as the rigid surface and the outer surface of the concrete core as the slave surface. The coefficient of friction between the two surfaces is chosen as 0.25. Hard Contact is provided between the two surfaces, which allows the pressure to be transmitted across the two surfaces only when there is actual contact among them, while causing the surfaces to separate under the influence of a tensile force.

2.3 Meshing

The Abaqus Standard module inset in ABAQUS is used for all analytical modeling purposes. The Abaqus Standard module consists of a comprehensive element library that provides different types of elements catering to different situations. Trials were performed with various element types such as Quad (C3D4), Wedge (C3D6) and Brick (C3D8). The C3D8 brick elements were found to be suitable for meshing both concrete and steel tube based on the accuracy as well as the computationa effort required.

2.4 Loading and Boundary conditions

The steel tube and the concrete core are left completely unrestrained in all directions to allow any possible deformation in the column. A rigid plate is attached at both the top and bottom of the model to simulate the platens in an actual testing machine.The bottom rigid plate is fixed completely using the encastre boundary condition applied at its reference node, while the loading was applied on the top rigid plate through displacement control (to simulate the strain controlled test).

3 RESULTS AND VALIDATION OF MODEL

The proposed model was used to numerically simulate different rectangular CFT columns from literature. The accuracy of the numerical model is evaluated based on the difference between the experimental and ABAQUS peak load capacities. The model must also be able to successfully capture the deformed shape of the composite member.The results of simulations for different authors are presented.

3.1 Schneider [7]

Schneider [7] tested six rectangular specimens (R1 through R6). All these specimens had a Length (L) to width (B) ratio (L/B) of 4 The specimens were filled with normal strength concrete. In the present study, the samples R2, R4, R5 and R6 were simulated. The dimensions and other details of the specimens are shown in Table 1(see Appendix). Fig. 1 represents the load deformation behavior (experimental vs ABAQUS) of some of these samples. A comparison of peak load capacities of all the samples is presented in Table 2(see Appendix).

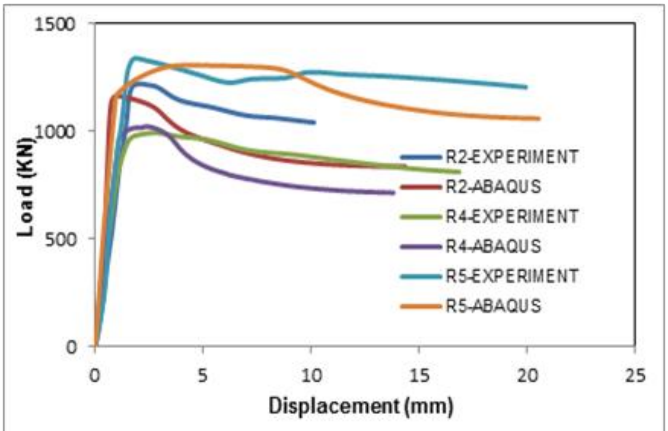

Fig.1 Comparison of experimental and numerical load-axial displacement behavior for specimens tested by Schneider

3.2 Liu et al [11]

Two samples, viz. C6-1 and C9-2 tested by Liu et al [11] were simulated. The sample properties are shown in Table 1(see Appendix). Fig. 2 compares the experimental and ABAQUS load-strain pattern for both the samples. From the results, it is clear that the numerical model is adequate to capture the compression behavior of the specimens. The experimental and numerical peak load values, as shown in Table 2(see Appendix), also display good agreement with each other.

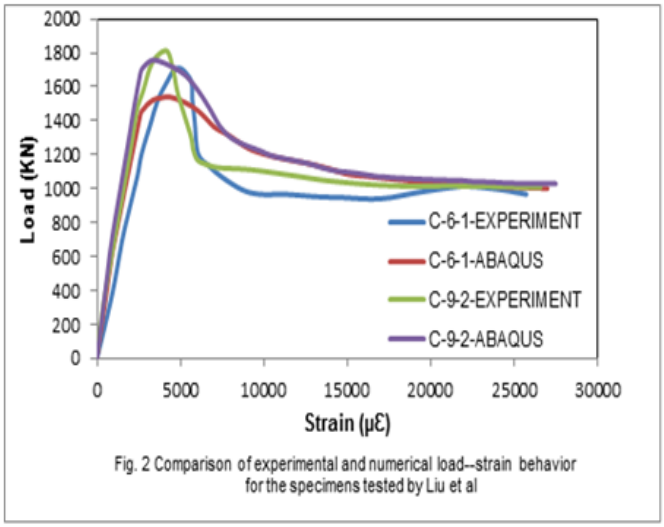

Fig. 2 Comparison of experimental and numerical load--strain behavior for the specimens tested by Liu et al

3.3 Liu et al [12]

Six samples tested by Liu et al [11] were simulated. The specimen labels and properties are shown in Table 1(see Appendix). Fig. 3 compares the experimental and numerically obtained deformed shapes for a typical rectangular specimen A5-1. Fig. 4 compares the experimental and ABAQUS load-strain behavior of these samples, while. It is clear that the numerical model agrees well with the experimental results for both these parameters.

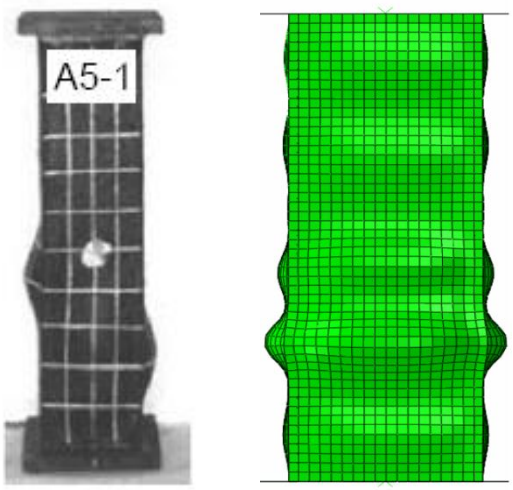

Fig. 3 Comparison of experimental deformed shape with deformed shape from ABAQUS for a typical column A5-1

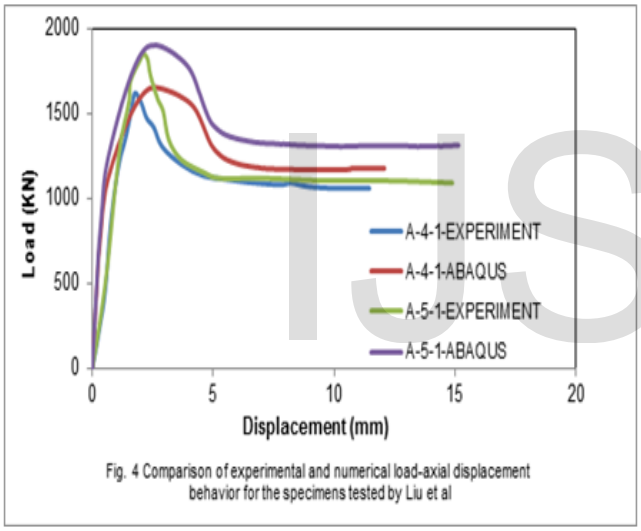

Fig. 4 Comparison of experimental and numerical load-axial displacement behavior for the specimens tested by Liu et al

3.4 Han [10]

Five samples tested by Han [10] were simulated. The specimen labels and properties are shown in Table 1(see Appendix). Fig. 5 compares the experimental and ABAQUS load-strain behavior of the samples rc6-1 and rc11-1. The peak axial load capacities for all the simulated specimens are shown in Table 2(see Appendix). From the table, it is clear that the load values obtained from ABAQUS generally show a good correlation with their experimental counterparts.

4 Conclusion

A nonlinear FEM based model has been developed using ABAQUS for the numerical simulation of rectangular CFT specimens. The proposed model is validated by comparing its output with the corresponding experimental data available in literature. The results (tabulated in Table 2) show that the proposed model is capable of reproducing the load-deformation behavior and deflected shape of the composite specimens. The model is found to work equally well for steel tubes filled with normal as well as high strength concrete, with the load capacities predicted by ABAQUS P_{abq} generally varying wit

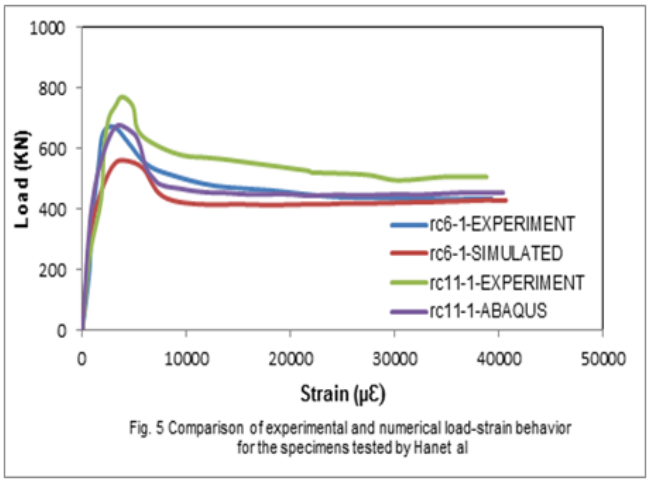

Fig. 5 Comparison of experimental and numerical load-strain behavior for the specimens tested by Hanet al

-hin ±5% of the corresponding experimental value $P_{exp.}$The average v -alue of P_{abq} / P_{exp} was obtained as 0.954, which indicates a good corr -elation between the experimental and numerically simulated results.

5 References

[1] ABAQUS 6.9 Documentation, ABAQUS User's and Analysis User's Manual 2009, Providence R.I

[2] N.E.Shanmugam and B.Lakshmi, "State of the art report on steel-concrete composite columns," Journal of Constructional Steel Research ,vol. 57 no.10, pp 1041-1080, Oct. 2007

[3] R.B. Knowles and R. Park," Strength of concrete filled steel tubular columns," Journal of Structural Engineering, vol. 95, no.12, pp 2565- 87, Dec.1969

[4] M. Tomii, K. Yoshimura, Y. Morishita, "Experimental studies on concrete-filled steel tubular stub columns under concentric loading," Proc. of the In -ternational Colloquium on Stability of Structures under Static & Dynamic Loads. Washington: SSRC/ASCE; pp. 718–41, 1977.

[5] H. Shakir-Khalil , M. Mouli, " Further tests on concrete-filled rectangular hollow-section columns," The Structural Engineer, vol. 68, no. 20, pp 405–13, 1990

[6] BS5400 Steel. Concrete and composite bridges: Part 5: Code of practice for design ofcomposite bridges, London: British Standards Institution, 1979

[7] S.P. Schneider, "Axially loaded concrete-filled steel tubes," Journal of Structural Engineering, ASCE, vol.124, no. 10, pp 1125-38, Oct. 1998

[8] H-T Hu et al. "Nonlinear analysis of axially loaded concrete-filled tubes with confinement effect," Journal of Structural Engineering, ASCE, vol.129, no. 10, pp 1322-29, Oct. 2003

[9] C. Huang et al., "Axial load behaviour of Stiffened concrete-filled Steel columns," Journal of Structural Engineering, ASCE, vol. 128, no. 9, pp 1222-1230, Sept. 2002

[10] L-H. Han, "Tests on stub columns of concrete-filled RHS sections," Jour -nal of Constructional Steel Resarch , vol. 58, no. 3, pp. 353-72, March 2002

[11] D. Liu, W-N. Gho, J. Yuan, "Ultimate capacity of high-strength rectangular concrete-filled steel hollow section stub columns," Jour nal of Construc -tional Steel Resarch , vol. 59, no. 12, pp. 1499-1515, Dec. 2003

[12] D. Liu, W-N. Gho, "Axial load behaviour of high-strength rectangular concrete-filled steel tubular stub columns," Thin-Walled Structures, vol. 43, no. 8, pp 1131-42, Aug. 2005

.

APPENDIX

TABLE 1
GEOMETRIC DETAILS AND MATERIAL PROPERTIES OF SIMULATED SPECIMENS

Specimen Label	Tested by	B (mm)	H (mm)	t (mm)	B/H	B/t	L (mm)	f_c (MPa)	f_y (MPa)	E_s (GPa)
R2	Schneider (1998)	152.8	76.5	4.47	2.0	34.18	611	26.044	383	213.59
R4		152.7	102.8	4.57	1.5	33.41	610	23.805	365	206.01
R5		151.4	101.3	5.72	1.5	26.47	606	23.805	324	204.63
R6		152.37	102.13	7.34	1.5	20.73	609	23.805	358	205.32
rc4-1	Han (2002)	150	135	2.86	1.1	52.45	450	59.30*	228	182
rc6-1		100	75	2.86	1.3	34.97	300	59.30*	228	182
rc8-1		140	105	2.86	1.3	48.95	420	59.30*	228	182
rc10-1		160	120	2.86	1.3	55.95	480	59.30*	194	194
rc11-1		130	85	2.86	1.5	45.45	390	59.30*	228	182
C6-1	Liu et al (2003)	119.6	80.6	4.18	1.5	28.61	360	60.8	550	207
C9-2		160.7	80.5	4.18	2.0	38.45	480	72.1	550	207
A-4-1	Liu et al (2004)	130	100	5.80	1.3	22.41	390	83	300	203
A-5-1		130	100	5.80	1.3	22.41	390	106	300	203
A-8-1		180	100	5.80	1.8	31.03	300	106	300	203
A-10-1		150	100	4.00	1.5	37.50	390	55	495	206
A-14-1		190	100	4.00	1.9	47.50	390	55	495	206

TABLE 2
COMPARISON OF NUMERICAL AND EXPERIMENTAL RESULTS

Specimen Label	Tested by	B/H	B/t	f_c (MPa)	Exp. Peak Axial Load P_{exp} (KN)	ABAQUS Peak Axial Load P_{abq} (KN)	P_{abq} / P_{exp}
R2	Schneider	2.0	34.18	26.044	1006	1021.54	1.015
R4	(1998)	1.5	33.41	23.805	1224	1164.06	0.951
R5		1.5	26.47	23.805	1335	1306.52	0.979
R6		1.5	20.73	23.805	1691	1629.69	0.964
rc4-1	Han (2002)	1.1	52.45	59.30*	1420	1188.09	0.837
rc6-1		1.3	34.97	59.30*	640	560.79	0.876
rc8-1		1.3	48.95	59.30*	1044	862.55	0.826
rc10-1		1.3	55.95	59.30*	1820	1607.87	0.883
rc11-1		1.5	45.45	59.30*	760	677.04	0.890
C6-1	Liu et al (2003)	1.5	28.61	60.8	1560	1541.43	0.988
C9-2		2.0	38.45	72.1	1820	1758.22	0.966
A-4-1	Liu et al (2004)	1.3	22.41	83	1601	1655.27	1.034
A-5-1		1.3	22.41	106	1854	1903.52	1.027
A-8-1		1.8	31.03	106	2287	2459.26	1.075
A-10-1		1.5	37.50	55	1815	1732.34	0.954
A-14-1		1.9	47.50	55	2038	2060.04	1.010
Average							0.954
Standard deviation							0.07328

* indicates the compressive strength of 150 mm cube; it must be noted that all other f_c values represent unconfined cylinder strength of concrete